Sub-Rayleigh optical vortex coronagraphy

E. Mari,[1,*] F. Tamburini,[2] G. A. Swartzlander Jr.,[3] A. Bianchini,[2] C. Barbieri,[2] F. Romanato,[4] and B. Thidé[5]

[1]*CISAS, University of Padua, I-35131 Padova, Italy*
[2]*Department of Astronomy, University of Padua, I-35122 Padova, Italy*
[3]*Chester F. Carlson Center for Imaging Science, Rochester Institute of Technology, Rochester, New York 14623, USA*
[4]*Department of Physics, University of Padua, I-35131 Padova, Italy*
[5]*Swedish Institute of Space Physics, P. O. Box 537, SE-751 21 Uppsala, Sweden*

[*]*elettra.mari@unipd.it*

Abstract: We introduce a new optical vortex coronagraph(OVC) method to determine the angular distance between two sources when the separation is sub-Rayleigh. We have found a direct relationship between the position of the minima and the source angular separation. A priori knowledge about the location of the two sources is not required. The superresolution capabilities of an OVC, equipped with an $\ell = 2$ N-step spiral phase plate in its optical path, were investigated numerically. The results of these investigations show that a fraction of the light, increasing with N, from the secondary source can be detected with a sub-Rayleigh resolution of at least $0.1\ \lambda/D$.

OCIS codes: (050.4865) Optical vortices; (100.6640) Superresolution; (050.1970) Diffractive optics; (350.1260) Astronomical optics.

References and links

1. A. Quirrenbach, "Coronographic Methods for the Detection of Terrestrial Planets," Arxiv preprint astro-ph/0502254 (2005).
2. F. Roddier and C. Roddier, "Stellar coronograph with phase mask," Publ. Astr. Soc. Pacif. **109**, 815–820 (1997).
3. D. Rouan, P. Riaud, A. Boccaletti, Y. Clénet, and A. Labeyrie, "The Four-Quadrant Phase-Mask Coronagraph. I. Principle," Publ. Astr. Soc. Pacif. **112**, 1479–1486 (2000).
4. D. Mawet, E. Serabyn, K. Liewer, R. Burruss, J. Hickey, and D. Shemo, "The vector vortex coronagraph: Laboratory results and first light at Palomar Observatory," Astrophys. J. **709**, 53–57 (2010).
5. G. Foo, D. M. Palacios, and G. A. Swartzlander, Jr., "Optical vortex coronagraph," Opt. Lett. **30**, 3308–3310 (2005).
6. J. Lee, G. Foo, E. Johnson, and G. A. Swartzlander, Jr., "Experimental verification of an optical vortex coronagraph." Phys. Rev. Lett. **97**(5), 053901 (2006).
7. E. Serabyn, D. Mawet, and R. Burruss, "An image of an exoplanet separated by two diffraction beamwidths from a star," Nature **464**(7291), 1018–1020 (2010).
8. P. Coullet, L. Gil, and F. Rocca, "Optical vortices," Opt. Commun. **73**(5), 403–408 (1989).
9. L. Allen, M. W. Beijersbergen, R. J. C. Spreeuw, and J. P. Woerdman, "Orbital angular momentum of light and the transformation of Laguerre-Gaussian laser modes," Phys. Rev. A **45**(11), 8185–8189 (1992).
10. F. Tamburini, G. Anzolin, G. Umbriaco, A. Bianchini, and C. Barbieri, "Overcoming the Rayleigh criterion limit with optical vortices," Phys. Rev. Lett. **97**(16), 163903 (2006).
11. D. Mawet, P. Riaud, O. Absil, and J. Surdej, "Annular groove phase mask coronagraph," Astrophys. J. **633**, 1191–1200 (2005).
12. G. A. Swartzlander, Jr., "The optical vortex coronagraph," J. Opt. A Pure Appl. Opt. **11**, 094022 (2009).
13. M. W. Beijersbergen, R. P. C. Coerwinkel, M. Kristensen, and J. P. Woerdman, "Helical-wavefront laser beams produced with a spiral phaseplate," Opt. Commun. **112**, 321–327 (1994).

#156392 - $15.00 USD Received 10 Nov 2011; revised 23 Dec 2011; accepted 26 Dec 2011; published 19 Jan 2012

14. E. Mari, G. Anzolin, F. Tamburini, M. Prasciolu, G. Umbriaco, A. Bianchini, C. Barbieri, and F. Romanato, "Fabrication and testing of *l = 2* optical vortex phase masks for coronography," Opt. Express **18**, 2339–2344 (2010).
15. E. Hecht, *Optics*, 4th ed. (Addison-Wesley Publishing Company, 2001).
16. H. Müller, S.-W. Chiow, Q. Long, C. Vo, and S. Chu, "Active sub-Rayleigh alignment of parallel or antiparallel laser beams," Opt. Lett. **30**, 3323–3325 (2005).
17. G. A. Swartzlander, Jr., "Peering into darkness with a vortex spatial filter," Opt. Lett. **26**, 497–499 (2001).
18. M. Pitchumani, H. Hockel, W. Mohammed, and E. Johnson, "Additive lithography for fabrication of diffractive optics," Appl. Opt. **41**(29), 6176–6181 (2002).
19. G. A. Swartzlander, Jr., "Obtaining spatial information from an extremely unresolved source," Opt. Lett. **36**, 4731–4733 (2011).
20. E. Mari, F. Tamburini, C. Barbieri, and A. Bianchini, "Fabrication and testing of phase masks for optical vortex coronagraph to observe extrasolar planets," Proceedings of SPIE 7735, 773534 (2010).

1. Introduction

The term coronagraph refers to an optical system that rejects the stellar light from a predefined area of the focal plane of a telescope in order to reduce associated speckle and photon shot noise [1]. In the search for extrasolar planets, the main problem is to suppress the diffracted starlight so as to reveal the presence of fainter nearby objects. Recent years have seen the development of several coronagraphic concepts characterized by different methods used to reject light from a given star [2–4]. The optical vortex coronagraph (OVC) [5–7] discussed here exploits particular screw dislocations, called optical vortices (OVs) [8] that are phase singularities embedded in helicoidal-wavefront light beams. Beams harbouring OVs carry an amount of orbital angular momentum (OAM) of $\ell\hbar$ per photon [9], where ℓ, called topological charge, indicates the number of interlaced helixes of the wavefront in one wavelength and $\hbar$ is Plank's reduced constant. Recently, Tamburini *et al.* [10] demonstrated that by exploiting the topological properties of OVs, the resolving power of any optical instrument can be improved by up to an order of magnitude below the Rayleigh criterion limit with white, incoherent light, and even up to fifty times when monochromatic and coherent sources are used. This is achieved by taking advantage of the asymmetric intensity of the peaks of the OVs.

In this paper we introduce, based on numerical simulations, an OVC criterion that utilizes the position of the minima of OVs with $\ell = 2$, to determine the angular separation between two sources even when they are unresolvable according to the Rayleigh criterion. We also provide the explicit evaluation of the efficiency of the detection of a secondary source. In this paper we do not approach the study of the use of higher topological charges that will be the subject of forthcoming study.

2. Optical vortex coronagraph

The OVC exploits the topological properties of even OVs to suppress the light from an on-axis source, thus making nearby fainter objects visible [5]. The choice of an even topological charge was found very advantageous [11,12] because only in this case OV presents an extended central zone of darkness instead of the point-like region of darkness as in the case for odd ℓ OV. This setup has provided striking proofs of the validity of this technique by imaging planets around a distant star with a vortex vectorial mask [7]. Figure 1 shows the optical scheme of an OVC.

There are different ways to impose optical vorticity on a light beam. In this paper we have simulated the insertion into in the optical path of a particular vortex lens, the spiral phase plate (SPP) [13]. The SPP is a transparent helicoidal plate whose thickness increases with the azimuthal angle φ. When the spiral shape of the SPP has a smooth, continuous, helicoidal pattern the phase of the light is modulated smoothly and continuously. This ideal continuous spiral phase plate (CSPP) imposes a topological charge ℓ onto the beam according to the formula

#156392 - $15.00 USD Received 10 Nov 2011; revised 23 Dec 2011; accepted 26 Dec 2011; published 19 Jan 2012

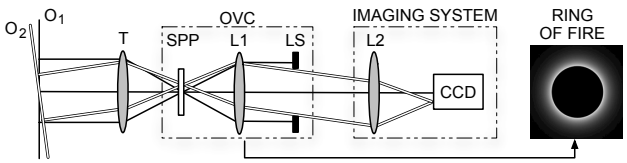

Fig. 1. Optical scheme of an OVC. T is the objective, L1 the collimating lens, and LS the Lyot stop, placed at the same focal distance as that of L1. The light of the on-axis object, O_1, crosses the central dislocation of the SPP and is transformed into a "ring of fire" in the back focal plane of L1. The ring of light is blocked by a Lyot stop LS placed in the back focal plane of L1. The light emitted by the off-axis source, O_2, evades the central dislocation of the SPP and the LS, so it is focused by L2 to be on the detector array CCD.

$\ell = (\Delta n \cdot h_s)/\lambda$ where h_s is the pitch of the CSPP, λ the wavelength of the incident light and Δn the difference between the refractive index of the SPP and that of the surrounding medium.

The stepped SPP is built like a spiral staircase with N discrete steps and is hereafter called multi-level SPP, MLSPP. Each of the steps introduces a constant phase shift in the light, imprinting an optical vorticity that is slightly different from that of a CSPP. So, the topological charge depends on the number of steps used to build the whole phase gap $\ell = [(\Delta n \cdot h_s)/\lambda][(N+1)/N]$, where N is an even integer [14]. For any integer value of the topological charge ℓ, the intensity profile of these vortices presents a doughnut-like shape. When the focused beam crosses the vortex lens far away from its optical singularity as an off-axis light source, it will behave as if it were crossing a simple slab of glass with the result that the intensity distribution of the beam would tend to preserve its original profile.

3. Sub-Rayleigh coronagraphy

The Rayleigh criterion describes the angular resolution of an optical system. It states that the Airy disks, i.e. the diffraction images of two separated mutually incoherent point-like sources, are resolved when the intensity maximum of one source overlaps the first intensity minimum of the second equally bright source. For a telescope having diameter D at wavelength λ, the separation is achieved at $\theta = 1.22\lambda/D$ [15]. Techniques to overcome this limit have been developed in certain special cases [16], and the idea of using an optical vortex mask to detect faint objects with sub-Rayleigh resolution has been suggested by Swartzlander [17] and Tamburini *et al.* [10]. In [17] the dark core of an optical vortex is used as a window to examine a weak background signal hidden in the glare of a bright source. In [10] the new sub-Rayleigh criterion is based on the measurement of the asymmetric peaks of intensity distribution of the off-axis source. We present a new criterion that exploits the position of a minima of the intensity profile generated by the off-axis source. We modeled two mutually incoherent monochromatic point sources, with the same wavelength, arranged at different angular separations. Observed by a diffraction-limited telescope, they would form two ideal Airy patterns that intersect the vortex lens at different transverse locations. Without vortex lens we should have the $\ell = 0$ case that for a single point source corresponds to the point spread function (PSF). When one of the source is aligned with the axis of the SPP, it forms a 'ring of fire' at the exit pupil plane (see Fig. 1), that then is ideally blocked from reaching the detector by the Lyot stop. A fraction of the light from the second off-axis source passes through the Lyot stop and is recorded on the detector. The fraction depends on the angular separation of the sources, the diameter of the Lyot stop, and the surface profile of the SPP. Here we assume the area of the Lyot stop to be one half the area of the ring of fire [6]. This change the resolution criterion to $1.22\lambda/D'$, where $D' = D/\sqrt{2}$.

Figure 2 shows the combined intensity distributions in the image plane for both sources,

#156392 - $15.00 USD Received 10 Nov 2011; revised 23 Dec 2011; accepted 26 Dec 2011; published 19 Jan 2012

and the corresponding horizontal profiles observed without and with the $\ell = 2$ SPP with 512 steps. The unresolved peaks in Fig. 2(a) are separated by an angular distance of $0.1\lambda/D'$. The

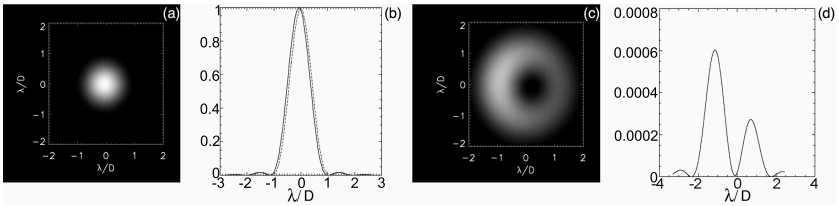

Fig. 2. Numerically generated intensity distributions and profiles (a) Two unresolvable point sources with the same intensity separated by $0.1\lambda/D$ (b) corresponding intensity profiles (c) Intensity pattern of the off-axis source when crosses an $\ell = 2$ SPP (see text) and its intensity profile (d).

asymmetric doughnut pattern in Fig. 2(c) is attributed to the small separation of the image of the second source on the SPP from the vortex axis. We have found that the minima of the profiles of the asymmetric doughnut pattern occur exactly at the angular separation when the separation is sub-Rayleigh. Figure 3 shows a plot of minima position versus angular separation and an example of image profile for one beam when the other sources is completely nulled by the OVC.

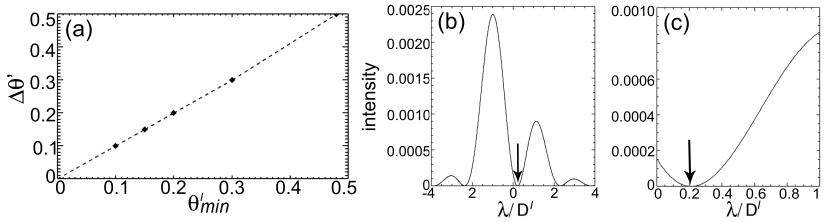

Fig. 3. (a): Plot of minima position versus angular separation. points represent numerically calculated examples. (b): Numerically generated intensity profile of one of two unresolvable point sources with the same intensity. Arrow indicate the minimum position θ_{min} for the angular separation $0.2\lambda/D'$. (c) Enlargement of the minimum zone of the profile (b). The minimum occur exactly at the angular separation $0.2\lambda/D'$.

Therefore, a reliable measure of the sub-Rayleigh angular distance between two controlled point sources can be determined by measuring the position of the minimum of the OV generated by the off-axis source with respect to the optical axis. The measured profiles are the sum of the residual light of the primary plus that of the secondary source and the minima are absolute minima. The average power within the dark vortex core (see for example Fig. 2(c)) is plotted in Fig. 4 for the case where the primary and secondary sources subtend a fixed angle of $\Delta\theta' = 0.3\lambda/D'$, and where the relative position of the axis of the SPP with respect to the primary source, $\Delta\theta'_{SPP}$ is varied. This corresponds to scanning the telescope across the sky and measuring the intensity within the vortex core on a CCD pixel. The plot demonstrates the correspondence between the minimum measured value(within the vortex core region) and the angle $\Delta\theta'$ when the primary is aligned with the SPP axis. The point $\Delta\theta'_{SPP} = 0$ corresponds to the alignment of the secondary source with the SPP axis. This plot shows that the position of the minimum power indicates the angular distance of the secondary source from the primary. In other words the absolute minimum is obtained when the primary is aligned with the SPP and, as a consequence, when $\Delta\theta' = \Delta\theta'_{SPP}$.

#156392 - $15.00 USD Received 10 Nov 2011; revised 23 Dec 2011; accepted 26 Dec 2011; published 19 Jan 2012

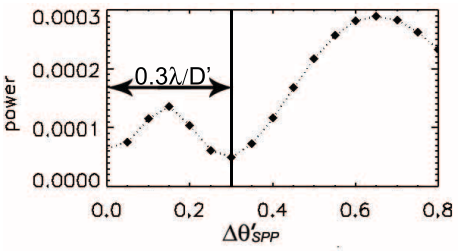

Fig. 4. Power measured in the dark vortex core region when the sources subtend a fixed angle $\Delta\theta' = 0.3\lambda/D'$ and when the telescope is swept through an angle, $\Delta\theta'_{SPP}$ (along a line defined by the two sources). The position $\Delta\theta'_{SPP} = \Delta\theta'$ corresponds to an alignment of the SPP axis and the primary star.

3.1. Numerical evaluation of the efficiency of detection of a secondary source

We have calculated the percentage of power of the off-axis source transmitted through the LS. From an experimental point of view it is important to consider the surface profile of the SPP when it is multi-stepped. We numerically examined the deviation from ideal results when $N = 8, 16, 64$ and 512. Note that the $N = 8$ MLSPP is the easiest to fabricate using lithographic methods [18]. The Interactive Data Language (IDL) software routines encoded and manipulated the images by using a set of 4096×4096 matrices, where the diameter of the Airy disks were encoded in 20 pixels, and the exit pupil in 256 pixels. When the Airy diffraction pattern intersects the SPPs, the IDL routine calculates the output image point by point using the Fourier imaging technique [12, 19]. The intensities of the stellar sources were normalized to unity. The secondary source is displaced in order to avoid that the center of the Airy disk falls on the highest step, i.e. the phase pitch. When the off-axis source is at sub-Rayleigh distance the Airy disk partially always cross the central singularity. Table 1 shows the numerical results obtained for different angular separations of the two sources. From the calculated percentage of light, we

Table 1. The percentage of the light of the secondary source passing through the LS with a diameter 0.7 times that of the exit pupil of the telescope. It depends on the number of the steps *N* used to build the total phase gap and on the angular distance $\Delta\theta$ in units of λ/D.

N \ $\Delta\theta'$	**0.1**	**0.2**	**0.5**	**1**	**1.22**	**1.5**	**2**	**3**
∞	0.58	2.36	15.39	56.94	74.25	88.17	97.25	100
512	0.57	2.35	15.37	56.84	74.13	88.17	97.16	100
64	0.54	2.28	15.21	56.16	73.25	87.42	96.31	100
16	0.52	2.06	13.94	51.72	67.76	81.39	90.09	98.99
8	0.49	1.99	10.78	40.07	53.32	69.98	79.22	95.37

see that the OVC has a transmission of up to 100% at angular separations larger than $3\lambda/D'$. A certain percentage of the light from the secondary source passes through the LS to be detected even below the Rayleigh criterion [10, 17]. We find that the amount of light increases with the number of steps of the SPPs.

3.2. Results in graphical form

In confirmation of the numerical results shown in the previous section, we present here, in graphical form, some results (Fig. 5) obtained in the image plane with our numerical simulations of Table 1, below and above the Rayleigh criterion limit. We have used different intensity

#156392 - $15.00 USD Received 10 Nov 2011; revised 23 Dec 2011; accepted 26 Dec 2011; published 19 Jan 2012

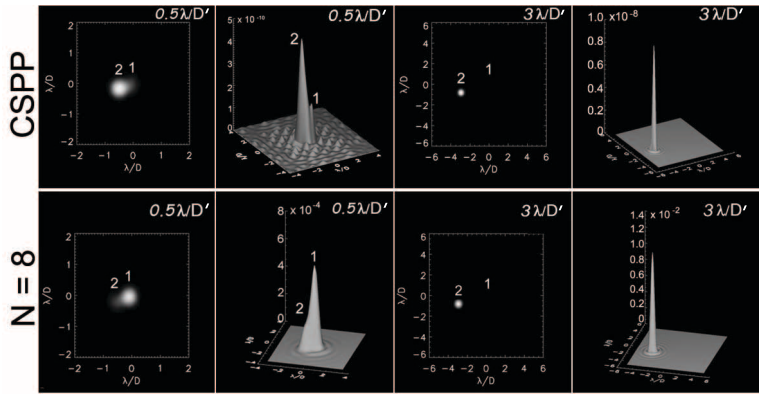

Fig. 5. Simulated coronagraphic image in 2D and 3D for an ideal SPP (upper panels) and a stepped SPP with 8 levels(lower panels), when the two sources have an intensity ratio of 10^-8 and 10^{-2}, respectively. Angular distances between two objects: $0.5\lambda/D'$ and $3\lambda/D'$.

ratios between two sources because each SPP has a different efficiency that depends on the number of steps [20]. For a CSPP, when the secondary source is at angular distance $0.5\lambda/D'$, a percentage of 15.4% of its light is visible. For an SPP with $N = 8$, when $\Delta\theta = 0.5\lambda/D'$, the percentage decreases to 10.78%. From these plots we see that at $\Delta\theta = 0.5\lambda/D'$ the coronagraphic image loses its symmetry because of the presence of the secondary source. In fact, the OV produced by the on-axis source is partially filled by a portion of the light of the fainter companion, revealing its presence. Our results suggest that the OVC could be applied to the detection of the unresolved companions in double systems and to the study of planets that are approaching the star before a transit, i.e. when the planet is at angular distance below the Rayleigh limit.

4. Conclusions

We have introduced a new criterion to determine the angular separation between two sources above sub-Rayleigh condition. We exploit the asymmetric intensity distribution of the OVs produced by a double system that crosses an $\ell = 2$ SPP, and we found that the distance from the optical axis of the absolute minimum of the intensity of the OV is equal to the angular separation between the two sources. Hence, measuring the displacement of the absolute minimum of the OV from the center, we can determine the sub-Rayleigh angular distance. This minimum is obtained when the telescope is pointing exactly at one of the sources. So, the exact position of the bright source does not need to be known a priori. This is a new criterion different from the ones proposed in [10] and [17]. In fact, those schemes require the measurement of the maxima of an intensity distribution, whereas we propose to exploit the positions of the absolute minima. We have also made a numerical study of the efficiency of the OVC simulating the separation of two sources at different angular distances with different $\ell = 2$ SPP. In the simulations the instrument was assumed to operate in the monochromatic regime. In all optical configurations considered, there is always a fraction of light from the fainter companion that becomes visible even below the Rayleigh criterion limit. The percentage of light from the secondary star passing through the LS increases with increasing angular separation. For this reason we suggest that OVC could be used as a pratical method to detect faint unresolved companions with ground-based and space-based telescopes, where the detrimental effects of the atmospheric turbulence do not affect the profile of the OVs. The possibility of observing solar systems below the Rayleigh criterion will open new frontiers in the study of planet transit.

#156392 - $15.00 USD Received 10 Nov 2011; revised 23 Dec 2011; accepted 26 Dec 2011; published 19 Jan 2012

Acknowledgments

This work has been partially supported by the University of Padova, by the Ministry of University and Research and by the CARIPARO Foundation.

#156392 - $15.00 USD Received 10 Nov 2011; revised 23 Dec 2011; accepted 26 Dec 2011; published 19 Jan 2012